



ARL-TR-9527 • AUG 2022



# **Development of a Python Module for Calculating Magnetization and Magnetically Influenced Phase Transformations**

**by Heather Murdoch, Efrain Hernandez, Anit Giri, and  
Daniel Field**

## **NOTICES**

### **Disclaimers**

The findings in this report are not to be construed as an official Department of the Army position unless so designated by other authorized documents.

Citation of manufacturer's or trade names does not constitute an official endorsement or approval of the use thereof.

Destroy this report when it is no longer needed. Do not return it to the originator.



# **Development of a Python Module for Calculating Magnetization and Magnetically Influenced Phase Transformations**

**Heather Murdoch, Efrain Hernandez, Anit Giri, and Daniel Field**  
*DEVCOM Army Research Laboratory*

REPORT DOCUMENTATION PAGE				Form Approved OMB No. 0704-0188	
<p>Public reporting burden for this collection of information is estimated to average 1 hour per response, including the time for reviewing instructions, searching existing data sources, gathering and maintaining the data needed, and completing and reviewing the collection information. Send comments regarding this burden estimate or any other aspect of this collection of information, including suggestions for reducing the burden, to Department of Defense, Washington Headquarters Services, Directorate for Information Operations and Reports (0704-0188), 1215 Jefferson Davis Highway, Suite 1204, Arlington, VA 22202-4302. Respondents should be aware that notwithstanding any other provision of law, no person shall be subject to any penalty for failing to comply with a collection of information if it does not display a currently valid OMB control number.</p> <p><b>PLEASE DO NOT RETURN YOUR FORM TO THE ABOVE ADDRESS.</b></p>					
<b>1. REPORT DATE (DD-MM-YYYY)</b> August 2022		<b>2. REPORT TYPE</b> Technical Report		<b>3. DATES COVERED (From - To)</b> October 2021–September 2022	
<b>4. TITLE AND SUBTITLE</b>  Development of a Python Module for Calculating Magnetization and Magnetically Influenced Phase Transformations				<b>5a. CONTRACT NUMBER</b>	
				<b>5b. GRANT NUMBER</b>	
				<b>5c. PROGRAM ELEMENT NUMBER</b>	
<b>6. AUTHOR(S)</b>  Heather Murdoch, Efrain Hernandez, Anit Giri, and Daniel Field				<b>5d. PROJECT NUMBER</b> AA7	
				<b>5e. TASK NUMBER</b> 05	
				<b>5f. WORK UNIT NUMBER</b>	
<b>7. PERFORMING ORGANIZATION NAME(S) AND ADDRESS(ES)</b>  DEVCOM Army Research Laboratory ATTN: FCDD-RLW-MF Aberdeen Proving Ground, MD 21005				<b>8. PERFORMING ORGANIZATION REPORT NUMBER</b>  ARL-TR-9527	
<b>9. SPONSORING/MONITORING AGENCY NAME(S) AND ADDRESS(ES)</b>				<b>10. SPONSOR/MONITOR'S ACRONYM(S)</b>	
				<b>11. SPONSOR/MONITOR'S REPORT NUMBER(S)</b>	
<b>12. DISTRIBUTION/AVAILABILITY STATEMENT</b>  Approved for public release: distribution unlimited.					
<b>13. SUPPLEMENTARY NOTES</b>  ORCID IDs: Heather Murdoch, 0000-0001-7710-0577; Efrain Hernandez, 0000-0002-7855-1027; Daniel Field, 0000-0002-8890-4391					
<b>14. ABSTRACT</b>  This report documents the Python module, MAGNETS.py, which was developed with the intention of modeling phase transformations in iron-based alloys under the influence of applied magnetic fields. The main requirement for such a model is the effect of the applied magnetic field on the free energy of each of the phases. The functions in the module determine the magnetic states of the phases, calculate the magnetization, and subsequently the change to the free energy. An example using the module shows the impact of an applied magnetic field on the martensite transformation.					
<b>15. SUBJECT TERMS</b>  magnetization, ferromagnetism, steel processing, martensite, CALPHAD, Sciences of Extreme Materials					
<b>16. SECURITY CLASSIFICATION OF:</b>		<b>17. LIMITATION OF ABSTRACT</b>	<b>18. NUMBER OF PAGES</b>	<b>19a. NAME OF RESPONSIBLE PERSON</b> Heather Murdoch	
<b>a. REPORT</b> Unclassified	<b>b. ABSTRACT</b> Unclassified	<b>c. THIS PAGE</b> Unclassified	UU	55	<b>19b. TELEPHONE NUMBER (Include area code)</b> (410) 306-0699

## Contents

---

---

<b>List of Figures</b>	<b>v</b>
<b>List of Tables</b>	<b>vi</b>
<b>1. Introduction</b>	<b>1</b>
1.1 Magnetic States	2
1.1.1 Ferromagnetic State: Magnetization	3
1.1.2 Paramagnetic State: Susceptibility	4
1.1.3 Antiferromagnetic State	5
1.2 Magnetic Properties of Alloys	5
1.3 Free Energy of a Phase	6
1.3.1 Internal Magnetic Energy	7
1.3.2 External Magnetic Energy	11
<b>2. Python Code</b>	<b>12</b>
2.1 Code Structure	12
2.1.1 Steel Class	14
2.1.2 Global Variables and General Functions	16
2.2 Functions for Alloy Properties	16
2.3 Functions for Free Energy of a Phase	20
2.3.1 CALPHAD Free-Energy Functions	21
2.3.2 Calculations for the Individual Phases	22
2.4 Functions for Internal Magnetic Energy Change	25
2.5 Functions for External Magnetic Energy change	28
2.5.1 Ferromagnetic State	28
2.5.2 Paramagnetic State	28
2.6 Functions for Magnetic States	31
2.6.1 Ferromagnetic State	31
2.6.2 Functions for Paramagnetic State	32
2.6.3 Functions for Antiferromagnetic State	34
2.7 Martensite Transformation Functions	35
2.7.1 $\gamma \rightarrow \alpha$ -martensite	35

2.7.2	$\gamma \rightarrow \epsilon$ -martensite	36
<b>3.</b>	<b>Examples</b>	<b>36</b>
3.1	Magnetization Curve and Susceptibility of Some Alloys	36
3.2	Free-Energy Curves	38
3.3	Martensite Transformation	39
<b>4.</b>	<b>Conclusions and Future Work</b>	<b>39</b>
<b>5.</b>	<b>References</b>	<b>41</b>
<b>Appendix A. MAGNETS.py*</b>		<b>44</b>
<b>Appendix B. MAGNETS_examples.ipynb*</b>		<b>45</b>
<b>List of Symbols, Abbreviations, and Acronyms</b>		<b>46</b>
<b>Distribution List</b>		<b>47</b>

## List of Figures

---

---

Fig. 1	Magnetization curves for pure iron calculated by WMFT (black dashed curve) and Kuz'min–Landau (magenta solid curve) for 0 Tesla. Experimental measurements are blue open circles. Under an applied field of 10 Tesla, experimental measurements are purple Xs <sup>1</sup> and the Kuz'min–Landau magnetization curve is magenta dashed line. ....	3
Fig. 2	The change in magnetic moment as a function of alloy content with the experimental measurements as points and the fits via Eq. 8 as dashed lines. The Fe-Ni system is an example of the fit needing multiple coefficients to capture the behavior of the magnetic moment as a function of Ni content, while the Fe-Mo system only needs one coefficient. ....	6
Fig. 3	The magnetization of pure iron calculated using the Kuz'min equations under no field (black curve) and under an applied field of 10 Tesla (blue curve). The new $T_C$ under the applied field is indicated by the red star at the inflection point of the magnetization curve.....	7
Fig. 4	(A) Example of issues with IHJ model in describing a material system with two magnetic states (ferromagnetic and antiferromagnetic) by using only one descriptor for the magnetic properties. (B) Xiong model fix for the issue by using two descriptors, one for each magnetic state. ....	10
Fig. 5	Visual representation of the integration of magnetization: the black curve is zero-field magnetization ( $M_z$ ), and the purple curve is magnetization under a magnetic field. At a given temperature, the zero-field magnetization is indicated by a black X and the magnetization under applied field indicated by a purple X. The field-induced magnetization ( $M_{fi}$ ) is the difference between the two, indicated by red arrow. ....	12
Fig. 6	Diagram of code structure. Python functions are in italics. Inputs to the functions are indicated by arrow bullet points. Subsidiary functions are regular bullet points. ....	13
Fig. 7	Diagram of ferromagnetic and paramagnetic models for $\alpha$ phase; experimental magnetization points at 10 Tesla are from Hao and Ohtsuka .....	23
Fig. 8	Plot of predicted susceptibility for the paramagnetic state of Fe-V. Experimental data as points from Arajs et al. and fit as lines from the <i>para_susceptibility()</i> function.....	37
Fig. 9	Example plot of magnetization curves at no field (navy) and an applied field of 20 Tesla (pink) using the <i>magnetization_curves()</i> function... 37	
Fig. 10	Plot of free-energy change from an applied field of 10 Tesla for the ferromagnetic $\alpha$ phase .....	38

Fig. 11	Plot of free-energy change from an applied field of 10 Tesla for the paramagnetic state of the antiferromagnetic $\gamma$ and $\epsilon$ phases .....	38
Fig. 12	Plot of shift in Ms temperature for both lath and plate forms from no field to an applied field of 10 Tesla for Fe-Mn alloys. Points are experimental observations from Stormvinter, and lines are the predicted Ms values from the <i>transformation_gamma_alpha()</i> function. ....	39

## **List of Tables**

---



---

Table 1	Attributes in class steel_class.....	14
Table 2	Global variables in MAGNETS.py module.....	16
Table 3	Keys in magnetic property dictionaries .....	20

## 1. Introduction

---

This report documents the Python module, *MAGNETS.py*, which was developed with the intention of modeling phase transformations under the influence of applied magnetic fields. The main requirement for such a model is the effect of the applied field on the free energy of the phase, which can generally be described by

$$\Delta G_{magnet} \propto -\mu_0 \int_0^H M(H, T, x) dH \quad (1)$$

where  $H$  is the applied field,  $\mu_0$  is the permeability of free space, and  $M$  is the magnetization, which is a function of the field, temperature ( $T$ ), and composition ( $x$ ).

Each phase will have a different magnetization, which, in addition to the factors described in Eq. 1, will also be dependent on the processing history of the material. Manipulation of the phase transformations through applied magnetic fields leverages the magnetization differences between the phases, which will be particularly distinct if the phases are in different magnetic states (e.g., one phase is ferromagnetic and the other is paramagnetic). This has been observed experimentally through the shift in the phase boundary for paramagnetic  $\gamma$ -austenite to ferromagnetic  $\alpha$ -ferrite in pure Fe<sup>1-4</sup> and Fe-Ni<sup>4</sup> and Fe-Co<sup>5</sup> binary alloys. Additionally, the start temperature of the paramagnetic  $\gamma$ -austenite to ferromagnetic  $\alpha$ -martensite was observed to shift under applied pulsed magnetic fields.<sup>6</sup> Even when the phases are of the same magnetic state (e.g., all ferromagnetic), differences in magnetization values can lead to reordering of the relative stability of phases, as observed in the formation of unexpected carbides during magnetic annealing.<sup>7,8</sup>

To calculate the magnetization and subsequent change to the free energy as a result of the applied magnetic field, the magnetic properties of the phase and alloy must be determined—in particular, the magnetic moment ( $\beta$ ) and the Curie temperature ( $T_C$ ) or Néel temperature ( $T_N$ ). The current module focuses on Fe-based alloys (e.g., steels), including a dictionary of magnetic properties for the  $\alpha$ -ferrite phase; however, the code is generalizable to other materials, as it is based around these obtainable material magnetic parameters.

In pure Fe it is straightforward to describe the magnetic state of a phase (e.g.,  $\alpha$ -Fe is ferromagnetic, with a transformation to paramagnetic at the  $T_C$  of 1043 K). In alloys, the magnetic state of each phase will vary depending on the composition and processing history. The magnetization will then vary by the phase, composition, processing history, and applied magnetic field. The code must account for the multiple possible magnetic states of the phases of interest.

## 1.1 Magnetic States

---

In general, magnetic properties of solids originate in the motion of electrons and in permanent magnetic moments of the atoms and electrons. There are two principal origins of the moments—one from the orbital motion of the electrons and the other from the electron spin. Among various magnetic states, paramagnetism, ferromagnetism, and antiferromagnetism are the states that are commonly found in Fe-based alloys. They arise due to the presence of permanent atomic or electronic magnetic moments.

Paramagnetism occurs when the magnetic moments are randomly oriented. Paramagnetic materials become magnetized when a magnetic field is applied but their magnetism vanishes upon removal of the applied magnetic field.

Ferromagnetism occurs when the magnetic moments are aligned in the same direction. Ferromagnets will tend to stay magnetized to some extent after being subjected to an applied magnetic field. Ferromagnetic materials possess a magnetic moment even in the absence of the applied magnetic field. This magnetization is called spontaneous magnetization. This magnetization is stable below the critical temperature  $T_c$ . Above this temperature the regular order of magnetic moment no longer exists (i.e., moments are randomly oriented). Then the ferromagnetic materials behave as paramagnets with no ordering of magnetic moments.

Antiferromagnetism occurs when the adjacent magnetic moments are oppositely directed and only one type of moment (same magnitude) is present so that the moments completely cancel out and the net moment is zero. The magnetization of antiferromagnetic materials is zero if there is no applied magnetic field. A small magnetization results if a field is applied. Further, the magnetization is orientation-dependent based on the location of the moments; the types of antiferromagnetism describe the expected locations of the oriented moments based on the crystal structure/sublattices. When heated, antiferromagnetic materials become paramagnetic at a critical temperature ( $T_N$ ).

Materials exhibiting paramagnetism, ferromagnetism, or antiferromagnetism are also generally referred to as belonging to the respective magnetic states (i.e., paramagnetic, ferromagnetic, or antiferromagnetic states, respectively). The following sections briefly describe the models/equations used to describe each of these states.

### 1.1.1 Ferromagnetic State: Magnetization

Kuz'min developed a magnetic equation of state for the ferromagnetic state (magnetic state below  $T_C$ ) for the ferromagnetic elements (Gd, Ni, Co, and Fe).<sup>9</sup> It is based on Landau theory relating magnetization to applied magnetic field and temperature. In previous work<sup>10</sup> some of the authors of this report modified the model to extend its application from pure elements to alloys. This extended model can then predict the magnetization of Fe-based alloys as a function of alloy content, temperature, and magnetic field. When compared with the results obtained using the well-known model based on Weiss Molecular Field Theory (WMFT), our modified model offered a significant improvement in terms of computational efficiency, extent of alloy space covered (i.e., it is not limited to dilute alloys), and accuracy compared with experimental data (Fig. 1). The expressions used in the model follow the figure.

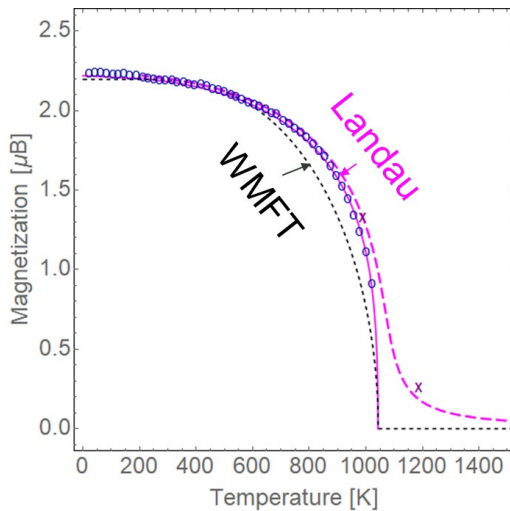


**Fig. 1** Magnetization curves for pure iron calculated by WMFT (black dashed curve) and Kuz'min–Landau (magenta solid curve) for 0 Tesla. Experimental measurements<sup>11</sup> are blue open circles. Under an applied field of 10 Tesla, experimental measurements are purple Xs<sup>1</sup> and the Kuz'min–Landau magnetization curve is magenta dashed line.

The applied field,  $H$ , is related to the magnetization,  $M$ , through the reduced magnetization,  $\sigma$  ( $M/M_0$ ), the reduced temperature  $\tau$  ( $T/T_C$ ), and the material specific fitting parameters  $a_0$ ,  $p$ , and  $\kappa$ :

$$H = a_0 \sigma \left[ \frac{\tau^3}{1 + p\tau^2} + \kappa \sigma^2 + (1 - \kappa) \sigma^4 \right] \quad (2a)$$

$$\sigma = \frac{M}{M_0} \quad (2b)$$

$$\tau = \frac{T}{T_C} = \left( \sqrt{1 - 2u + p^2 u^2} - pu \right)^{2/3} \quad (2c)$$

$$u = \frac{1}{2} \left[ \kappa \sigma^2 + (1 - \kappa) \sigma^4 - \frac{H}{a_0 \sigma} \right] \quad (2d)$$

$M_0$  is the saturation magnetization (directly related to magnetic moment), and  $T_C$  is the Curie temperature. Further details can be found in Murdoch et al.<sup>10</sup>

### 1.1.2 Paramagnetic State: Susceptibility

#### 1.1.2.1 Ferromagnetic Phase

As mentioned earlier, above the Curie temperature, ferromagnetic materials lose the regular ordering of the magnetic moment and transform to the paramagnetic state. The paramagnetic Curie temperature ( $\theta$ ) is another concept that has been used to describe the magnetic ordering temperature. It is found by fitting the measured inverse susceptibility in the paramagnetic state using the Curie–Weiss law

$$\chi = \frac{C}{T-\theta} \quad (3)$$

where  $\chi$  is the susceptibility,  $C$  is the Curie constant, and  $T$  is the temperature. The paramagnetic Curie temperature is usually higher than the Curie temperature. (For example,  $T_C = 1043$  K for pure  $\alpha$ -Fe where  $\theta = 1078$  K<sup>12</sup>).

To model the magnetic behavior in the paramagnetic state, the following expression has been employed using the Curie–Weiss parameters in the WMFT framework,<sup>10</sup> where

$$C = \frac{N_{AV}\{\beta_{alloy}\}^2(j+1)}{3kj} \quad (4)$$

Therefore, the susceptibility is

$$\chi = \frac{N_{AV}\{\beta_{alloy}\}^2(j+1)}{3kj(T-\theta)} \quad (5)$$

where  $N_{AV}$  is Avogadro’s number,  $k$  is Boltzmann’s constant,  $j$  is the Weiss molecular field theory parameter, which is 1 for paramagnetic materials, and  $\beta$  is the magnetic moment of the alloy.

#### 1.1.2.2 Antiferromagnetic Phase

For antiferromagnetic materials, the phase will also transform to the paramagnetic state above the  $T_N$ . The susceptibility is described by a slightly different form:

$$\chi = \frac{N_{AV}}{3k} \frac{\{\beta_{alloy}\}^2}{(T-\theta)} \quad (6)$$

where the parameters are the same as those previously described.

Here, however,  $\theta$  can be considered as function of the  $T_N$  that is dependent on the type of antiferromagnetism. This type is related to the crystal structure, as the magnetic spins are considered relative to their potential locations on the lattice/sublattices.

### 1.1.3 Antiferromagnetic State

The current version of the code does not consider the effect of magnetic field on the antiferromagnetic state due to the complexities that arise from orientation dependence and the fact that the  $T_N$  is often below room temperature and not a traditionally viable processing space. There are, however, placeholder functions in the code module for future work.

## 1.2 Magnetic Properties of Alloys

---

In the equations for the magnetic states, the material-specific magnetic properties are the magnetic moment ( $\beta$ ) and the magnetic transformation temperatures ( $T_C$ ,  $T_N$ ,  $\theta$ ). For an alloy these can generally be described as a combination of the values for the pure metals plus a series of interaction terms. In the CALculation of PHAses DiagrAmS (CALPHAD) methodology, the following polynomial forms are used<sup>13</sup>:

$$T_C^{Fe-X} = T_C^{Fe}x_{Fe} + T_C^Xx_X + x_{Fe}x_X \sum_{i=0}^n a_i \cdot (x_{Fe} - x_X)^i \quad (7)$$

$$\beta^{Fe-X} = \beta_{Fe}x_{Fe} + \beta_Xx_X + x_{Fe}x_X \sum_{i=0}^n b_i \cdot (x_{Fe} - x_X)^i \quad (8)$$

where Eq. 7 for  $T_C$  could also be used for  $T_N$  or  $\theta$ .

The terms  $x_{Fe}$  and  $x_X$  are the composition (in atomic fraction) of Fe and the alloying element,  $X$ , respectively. (This equation can be extended to ternary and other multi-component elements with the addition of their pure and interaction terms.) The interaction coefficients,  $a_i$  or  $b_i$ , are determined by fits to experimental magnetic property data and integration with the overall calculation of known phase boundaries for the alloy system. Each system may have variable numbers of coefficients,  $n$ , depending on what is required for a good fit. For example, an alloy with a complex variation in magnetic property could require three coefficients, whereas a simple linear relation could require no coefficients, just the pure value endpoints. Figure 2 shows two such example systems for the variation in  $\beta$  as a function of alloy content.<sup>13</sup>

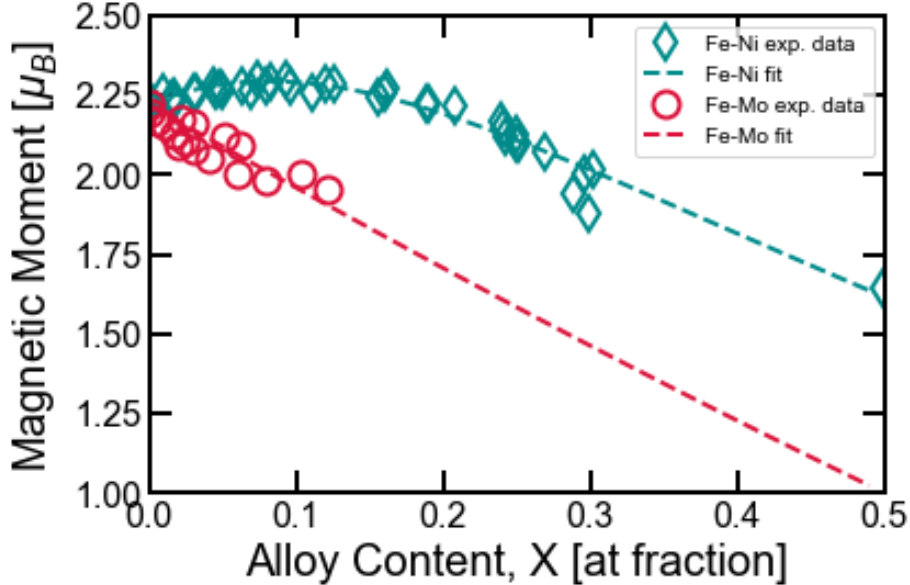


**Fig. 2** The change in magnetic moment as a function of alloy content with the experimental measurements as points and the fits via Eq. 8 as dashed lines. The Fe-Ni system is an example of the fit needing multiple coefficients to capture the behavior of the magnetic moment as a function of Ni content, while the Fe-Mo system only needs one coefficient.

These coefficients are currently tabulated for many iron-based systems in literature (e.g., Murdoch et al.<sup>13</sup>) and/or in software databases. However, as will be discussed in more detail in Section 1.3.1, these tabulated coefficients were often optimized as part of the whole phase diagram calculation and may not be the best fit specifically to the magnetic property data. Some systems where this occurs are Fe-Mn,<sup>14</sup> Fe-Cr,<sup>15</sup> and Fe-Co<sup>16</sup>; for example, in the Fe-Co system,  $1.35 \mu_B$  is used in the CALPHAD database for the magnetic moment of pure Co despite experimental observations of approximately  $1.8 \mu_B$ .<sup>16</sup>

### 1.3 Free Energy of a Phase

The general approach to describing the total free energy of a phase under an applied magnetic field is

$$G^{phase} = G_{non-mag} + G_{mag}^{int} + G_{mag}^{ext}$$

The nonmagnetic and internal magnetic terms are described by polynomial fits using the CALPHAD method and are available in commercial software (e.g., Thermo-Calc, JMatPro), open-source (e.g., pycalphad) databases, and literature.

The contributions of an applied field on the free energy of a phase include the following:

- The chemical/nonmagnetic term,  $G_{non-mag}$ , will not change with applied field.
- The internal magnetic energy term,  $G_{mag}^{int}$ , will be affected by an applied field.
- The external magnetic energy term,  $G_{mag}^{ext}$ , exists only in the presence of an applied field.

In the following sections we describe the details of how  $G_{mag}^{int}$  and  $G_{mag}^{ext}$  are affected under an applied magnetic field.

### 1.3.1 Internal Magnetic Energy

The internal magnetic energy term is related to the energy benefit to magnetic ordering (i.e., the difference between ferromagnetic and paramagnetic states). It is derived from the magnetic contribution to the heat capacity. The general form for this term is a piecewise function with the split condition at the magnetic transition temperature (either Curie or Néel). As this transition temperature can change under applied field, the internal magnetic energy can also change. The change in T<sub>c</sub> under an applied magnetic field is fairly straightforward and can be calculated from the inflection point on the magnetization curve, identified by the red star in Fig. 3. The application of a magnetic field increases the T<sub>c</sub>.

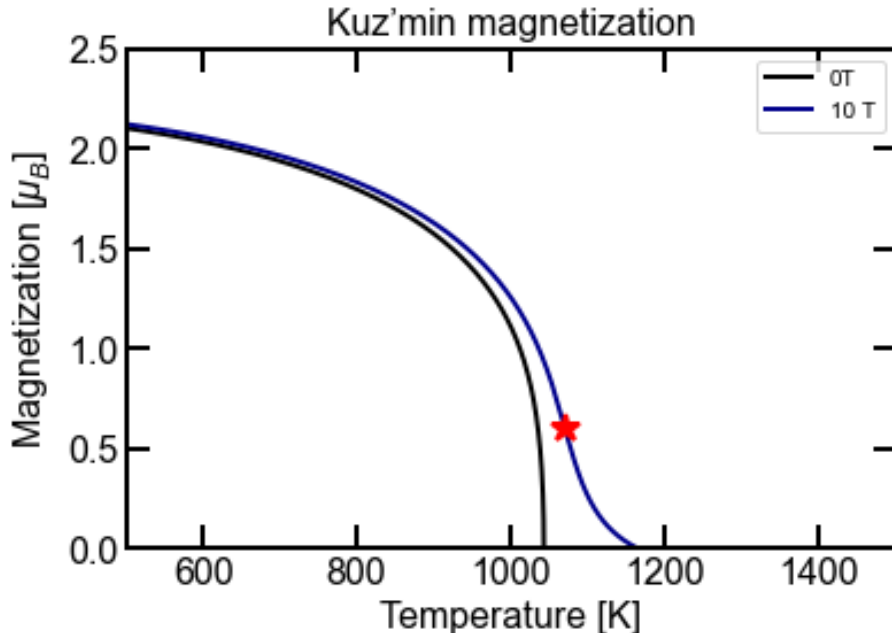


**Fig. 3** The magnetization of pure iron calculated using the Kuz'min equations under no field (black curve) and under an applied field of 10 Tesla (blue curve). The new T<sub>c</sub> under the applied field is indicated by the red star at the inflection point of the magnetization curve.

That the internal magnetic energy changes under an applied field in a ferromagnetic material is borne out by experimental observations of the heat capacity in Fe and Ni.<sup>17–19</sup> Under an applied magnetic field, the heat capacity curves generally exhibit a more diffuse peak and higher measured values at higher temperatures. In particular, Gschneidner and Pecharsky<sup>19</sup> calculated the magnetic entropy from their experimental heat capacity measurements and found it to increase under an applied field. Modeling of the heat capacity using spin-lattice dynamics showed similar behavior.<sup>20</sup>

Unfortunately, there are no straightforward approaches to determining the influence an applied field has on the  $T_N$ . Morrish<sup>21</sup> states that an applied field will lower the  $T_N$ , but this is based upon a scenario where the field is applied parallel to a particular sublattice in a given crystal structure. Experimental studies show both decreases and increases in  $T_N$  depending on the orientation of the field vis-à-vis the sample.<sup>22,23</sup> Boersma et al. showed a decrease in the Néel (approximately  $-0.2^\circ$  K/Tesla) when the field was applied along the easy axis and an increase when applied along the hard axes.<sup>22</sup> Christian et al. showed a similar orientation trend. Both studies showed about a  $0.1^\circ$ – $0.2^\circ$  change in the  $T_N$  per Tesla.<sup>23</sup> Conversely, the  $T_N$  in various orientations of single-crystal Cr was found to not vary at all ( $\pm 0.01^\circ$ ) in fields up to 10 Tesla<sup>24</sup> or up to 16 Tesla ( $\pm 0.02^\circ$ ).<sup>25</sup>

In our approach, we would generally consider polycrystalline samples, where even a strong textural component is not comparable to a single orientation crystal. As such, even if there were a change to the  $T_N$  as a function of orientation, it would be countered by the multiple grain orientations. Therefore, we elect to neglect any change to the  $T_N$  with applied field.

In summary, we expect the internal magnetic free energy of a phase to change under an applied field if it has a ferromagnetic state (i.e., the  $T_C$  will be affected), but not if it has an antiferromagnetic state.

The specific equations for the internal energy terms are discussed in the following. The most common model is the formulism by Inden–Hiller–Jarl (IHJ).<sup>26,27</sup> However, note that it has known drawbacks with respect to alloys that contain multiple magnetic states depending on composition range. A more recent model by Xiong et al.<sup>28</sup> addressed these concerns and is used in this code. We describe both forms here and have functions for both, as it is necessary to switch from the IHJ to Xiong form for some systems (e.g., Fe-Cr, which is ferromagnetic on the Fe-rich end and antiferromagnetic on the Cr-rich end).

### 1.3.1.1 IHJ Model

The internal magnetic free energy of the IHJ model is described by

$$G_{internal}^{magnetic} = R T \ln(\beta_{avg} + 1) g(\tau) \quad (9)$$

where  $\tau$  is the same as defined previously,  $\beta_{avg}$  is the average magnetic moment, and  $g(\tau)$  is

$$g(\tau) = \begin{cases} 1 - \frac{1}{A} \left[ \frac{79\tau^{-1}}{140p} - \frac{474}{497} \left( \frac{1}{p} - 1 \right) \left( \frac{\tau^3}{6} + \frac{\tau^9}{135} + \frac{\tau^{15}}{600} \right) \right], & \tau < 1 \\ -\frac{1}{A} \left[ \frac{\tau^{-5}}{10} + \frac{\tau^{-15}}{315} + \frac{\tau^{-25}}{1500} \right], & \tau \geq 1 \end{cases} \quad (10)$$

with  $A$  as a constant:

$$A = \frac{518}{1125} + \frac{11692}{15975} \left( \frac{1}{p} - 1 \right) \quad (11)$$

and  $p$  is an empirically derived ratio of magnetic enthalpy due to short range order relative to the total magnetic enthalpy, and is given by

$$p = \begin{cases} 0.4, & \text{for BCC} \\ 0.28, & \text{for FCC and HCP} \end{cases} \quad (12)$$

which was originally determined via experimental data from pure Fe and pure Ni, respectively.<sup>26</sup>

In several systems, such as Fe-Cr, there is both a ferromagnetic and an antiferromagnetic phase. The IHJ formulism applies a prefactor to the magnetic property equations (Eqs. 7 and 8) based on crystal structure (-1 for body-centered cubic and -3 for face-centered cubic/hexagonal close-packed) to capture the antiferromagnetic phase. This severely constrains the description for the  $T_N$  as a function of composition to maintain a continuous function across the whole composition range. This is depicted in Fig. 4A, where the  $T_N$  description is obviously a poor fit for any of the antiferromagnetic state (purple points) besides the endpoint. An improvement by Xiong et al.<sup>28</sup> separates the descriptions for the ferromagnetic and antiferromagnetic states (e.g., here the  $T_N$  and  $T_C$  (Fig. 4B). However, the Xiong model does require the use of local magnetic moments, which are scarce in the literature.

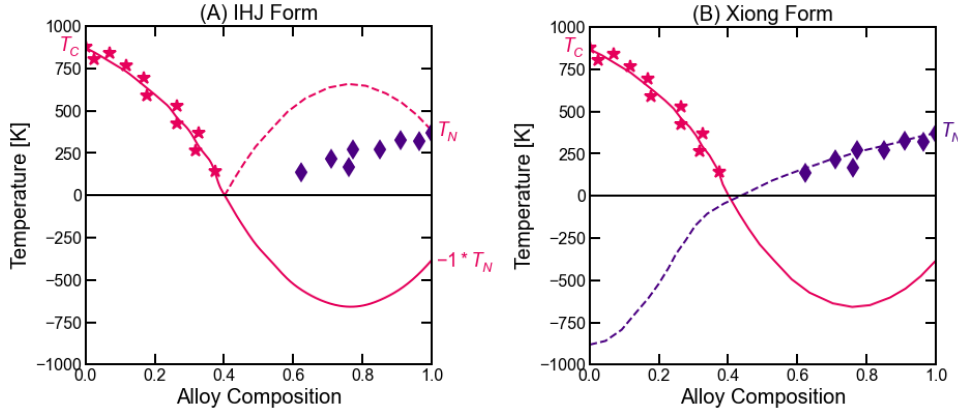


**Fig. 4** (A) Example of issues with IHJ model in describing a material system with two magnetic states (ferromagnetic and antiferromagnetic) by using only one descriptor for the magnetic properties. (B) Xiong model fix for the issue by using two descriptors, one for each magnetic state. (Figure adapted from Xiong et al.<sup>28</sup>)

### 1.3.1.2 Xiong Model

Xiong et al.<sup>28</sup> developed a revised magnetic model using a thermodynamic effective magnetic moment,  $\beta^*$ , to address the issues in alloys with both ferromagnetic and antiferromagnetic phases. This effective magnetic moment is calculated as follows:

$$\beta^* = \prod_i (\beta_i + 1)^{x_i} - 1 \quad (13)$$

and then used in the free energy as follows:

$$G_{internal}^{magnetic} = R T \ln(\beta^* + 1) g(\tau) \quad (14)$$

where  $g(\tau)$  is refit:

$$g(\tau) = \begin{cases} 1 - \frac{1}{D} \left[ 0.38438376 \frac{\tau^{-1}}{p} - 0.63570895 \left( \frac{1}{p} - 1 \right) \left( \frac{\tau^3}{6} + \frac{\tau^9}{135} + \frac{\tau^{15}}{600} + \frac{\tau^{21}}{1617} \right) \right], & 0 < \tau \leq 1 \\ -\frac{1}{D} \left[ \frac{\tau^{-7}}{21} + \frac{\tau^{-21}}{630} + \frac{\tau^{-35}}{2975} + \frac{\tau^{-49}}{8232} \right], & \tau > 1 \end{cases} \quad (15)$$

where  $D$  is a constant:

$$D = 0.33471979 + 0.49649686 \left( \frac{1}{p} - 1 \right) \quad (16)$$

and  $p$  is also refit to

$$p = \begin{cases} 0.37, & \text{for BCC} \\ 0.25, & \text{for FCC and HCP} \end{cases} \quad (17)$$

Note that the local moments for antiferromagnetic materials can be negative for a portion of the composition range—the values used for Eq. 13 are the absolute value.

The existing CALPHAD database fits for the magnetic moment have been optimized to fit the magnetic contribution to the specific heat rather than the absolute measured values of the magnetic moment. Since these fits have been optimized specifically in the context of the contribution to the internal free energy, it is rational to continue to use these adjusted thermodynamic moments for the description of how the internal free energy,  $G_{mag}^{int}$ , will change with an applied field. However, in calculating the external free-energy contribution,  $G_{mag}^{ext}$ , the existing adjusted parameters should not be used, as we desire an accurate description of the moment for use in the magnetization/susceptibility calculation.

Returning to the impact of an applied magnetic field, for either the IHJ or Xiong model, the shift in  $T_c$  expected under an applied field will affect the reduced temperature input,  $\tau$ , and subsequently the internal magnetic energy.

### 1.3.2 External Magnetic Energy

The external term for the effect of an applied magnetic field on the free energy is

$$G_{mag}^{ext} = -\mu_0 \int_0^H M(H, T, x) dH \quad (18)$$

where  $H$  is the applied field and  $M$  is the magnetization, which is a function of the field, temperature ( $T$ ), and composition ( $x$ ), and  $\mu_0$  is the permeability of free space.

For ferromagnetic states this is evaluated as

$$G_{mag}^{ext} = -\mu_0 \left( M_{zf} + \frac{1}{2} M_{fi} \right) H \quad (19)$$

where  $M_{zf}$  is the zero-field magnetization and  $M_{fi}$  is the field-induced magnetization. The components of the magnetization are illustrated in Fig. 5.

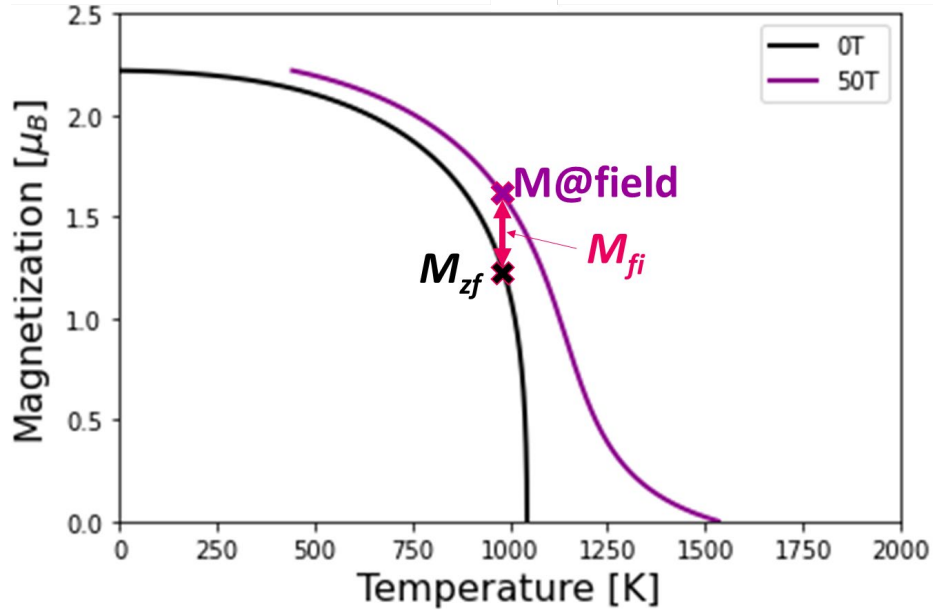


**Fig. 5** Visual representation of the integration of magnetization: the black curve is zero-field magnetization ( $M_z$ ), and the purple curve is magnetization under a magnetic field. At a given temperature, the zero-field magnetization is indicated by a black X and the magnetization under applied field indicated by a purple X. The field-induced magnetization ( $M_{fi}$ ) is the difference between the two, indicated by red arrow.

For paramagnetic states Eq. 18 becomes

$$G_{mag}^{ext} = -\mu_0 \frac{1}{2} \chi H^2 \quad (20)$$

where  $\chi$  is the susceptibility calculated either via Eq. 5 or Eq. 6 depending on whether the material has an antiferromagnetic state or not. Antiferromagnetic states (below the  $T_N$ ) are out of the scope of this work, being so depending on the crystal structure of the phase and the orientation of the field, among other factors.

## 2. Python Code

---

### 2.1 Code Structure

---

The overall structure of the code is delineated in Fig. 6 and the code itself is in Appendix A. The overarching function *magnet\_energies()* returns the free-energy descriptions for all phases of interest by calling the phase-specific functions that calculate the contributions to the free energy from the magnetic field and the Thermo-Calc function, *alpha\_gamma\_epsilon\_energy()*, for the nonmagnetic components. To calculate the martensitic phase transformations, the summary free energies are passed to *transformation\_gamma\_alpha()* for the  $\gamma \rightarrow \alpha$ -martensite

transformation and *transformation\_gamma\_epsilon()* for the  $\gamma \rightarrow \epsilon$ -martensite transformation.

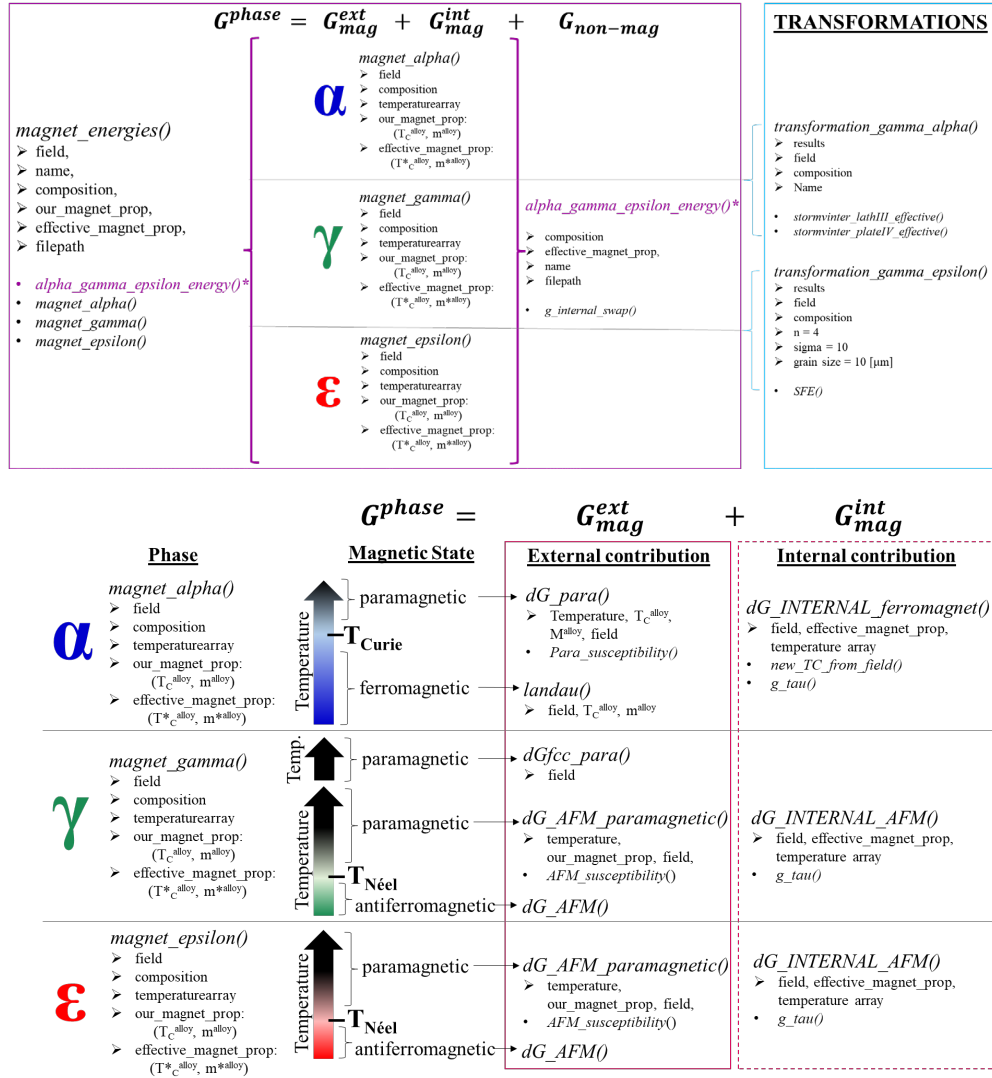


**Fig. 6 Diagram of code structure. Python functions are in italics. Inputs to the functions are indicated by arrow bullet points. Subsidiary functions are regular bullet points.**

Each phase (for steel:  $\alpha$ ,  $\gamma$ ,  $\epsilon$ ) has its own summarizing function—*magnet\_alpha()*, *magnet\_gamma()*, and *magnet\_epsilon()*—within which decisions are made about how to calculate the contribution to the free energy associated with the applied field. These are split between the contributions to the external energy,  $G_{\text{mag}}^{\text{ext}}$ , and to the internal energy,  $G_{\text{mag}}^{\text{int}}$ . At each temperature considered, the magnetic state of the phase is determined (e.g., by comparison to the magnetic transition temperature of the phase), and the function associated with that magnetic state is called to calculate the free-energy change.

These functions are all contained in the module: MAGNETS.py and called by the various example scripts. The Python class **steel\_class** is in the module and used to store all the necessary information about the alloy.

### 2.1.1 Steel Class

The steel class is initialized with a name for the alloy to be investigated, a dictionary of the alloy composition, and the unit for the composition dictionary. The composition dictionary has the elements as the keys and the amount as the value. The values can either be in units of weight percent (wt%), weight fraction (wt), atomic percent (at%), or atomic fraction (at). The class automatically converts the initialized composition unit type to the other three unit types for ease of calculations later. Generally, the magnetic calculations take in composition in atomic fraction, while the thermodynamic calculations take in weight percent. The other attributes of the class are in Table 1 and include dictionaries for the magnetic properties of the alloy (*mag\_prop*, *effective\_mag\_prop*, and *calphad\_mag\_prop*), which will be further discussed in Section 2.2, a dictionary for the free energy of phases (*dG*) to be discussed in Section 2.3, and a dictionary for the martensite start temperatures (*Ms*) to be discussed in Section 2.7.

**Table 1 Attributes in class steel\_class**

Attribute	Type	Format	Value unit	Example
Name	String	Name	...	'Fe_0.1C_5Ni'
comp_WT_percent	Dictionary	{'element': value}	wt% <sup>a</sup>	{'C': 0.5, 'Cr': 12}
comp_WT_fraction			wt	
comp_AT_percent			at%	
comp_AT_fraction			at	
molar_mass	Float	Float	g/mol	55.8
mag_prop	Dictionary	{'phase': 'm': moment, 'Tc': Curie/Néel temperature}	m: $\mu_B$ Tc: K	{'bcc': 'm': 2.1, 'Tc': 1037}
effective_mag_prop	Dictionary	{'phase': 'm': moment, 'Tc': Curie/Néel temperature}	m: $\mu_B$ Tc: K	{'bcc': 'm': 1.97, 'Tc': 1032}
calphad_mag_prop	Dictionary	{'phase': 'm': moment, 'Tc': Curie/Néel temperature}	m: $\mu_B$ Tc: K	{'bcc': 'm': 2.22, 'Tc': 1043}
dG	Dictionary	{'phase': [free energy array], 'T [K]': [temperature array]}	J/mol K	{'bcc': [1000, ..., 60000], 'fcc': [2000, ..., 50000], 'T [K]': [1, ..., 1000] }

Ms	dictionary	{‘type’: temperature}	K	{‘exp’: 437, ‘ab3’: 468}
----	------------	-----------------------	---	--------------------------

<sup>a</sup>Composition can be passed into the class in any of the four options for units; the class converts the passed in unit to the other three units.

## 2.1.2 Global Variables and General Functions

Variables and functions in this section are utilized in several locations throughout the code. The variables are delineated in Table 2 and include physical constants, materials parameters, and conversion factors.

**Table 2 Global variables in MAGNETS.py module**

Variable	Value	Unit	Description
mu0	$4\pi 1e-7$	Wb/(A m)	$\mu_0$ , Permeability
muB	9.274e-24	J/T	$\mu_B$ , Bohr magneton
k	1.38e-23	J/K	Boltzmann constant
Nav	6.02214076e23	/mol	Avogadro's number
R	8.314	J/(K mol)	Gas constant
mm	'Fe':55.845, 'C':12.0107, 'Mn':54.938, ...	g/mol	Molar mass
teslaconvert	7.958e5	Tesla → A/m	Conversion factor for magnetic field units $1 [T] = 10^4 [Oe]$ and $\frac{4\pi}{1000} [Oe] = 1 \left[\frac{A}{m}\right]$
cmg_to_mkg	$4\pi 1e-3$	$cm^3/g \rightarrow$ $m^3/kg$	Conversion factor for susceptibility units
magnetred	(0.902, 0, 0.357)	RGB	Color values for plots,
alphacolor	(0, 0, 1)		for each by phase
gammaacolor	(0.2, 0.6, 0.4)		
epsiloncolor	(1, 0, 0)		

Note: RGB = red–green–blue

*find\_nearest(array, value)*

### Purpose

- finds the nearest value in an array to a specified value

### Parameters

- array: array of interest
- value: value to find in the array

### Returns

- idx: index of array nearest to value

## **2.2 Functions for Alloy Properties**

---

There are two main functions for calculating the change to the magnetic properties as a function of alloy content:

- *alloy\_curiel\_neel()*
- *alloy\_moment()*

A third function, *moment\_effective()*, is used in the process of generating the alloy coefficients from local moments for the effective moment in Eq. 13. Two empirical equations for  $T_N$  are included from Aristeidakis and Haidemenopoulos<sup>29</sup> in functions as well.

Within each function are the dictionaries of coefficients to describe the change in  $T_C$ ,  $T_N$ , or magnetic moment (here,  $\beta$ ). The coefficients are in the form of Eqs. 7 and 8 from Section 1.2 with the composition in atomic fraction.

The same coefficients for the  $T_C$  would be used for the paramagnetic  $T_C$ ; however, the value for pure Fe used would be 1078 or 1093 K<sup>12</sup> for paramagnetic  $T_C$  instead of 1043 K for  $T_C$ . We have two instantiations of the alloy descriptions, one for the internal free energy (that may use adjusted/effective property values) and one for the external free energy (which is the most accurate fit to the experimentally observed property values). The Xiong internal energy model uses an effective magnetic moment by definition. Therefore, there are separate dictionaries for the effective property fits used for the internal energy calculation versus the property fits for the external energy calculation.

The keys for the coefficient dictionaries are the following:

- phase
  - element
    - $i$                        $i$ th coefficient value
    - *pureX*               $T_C^X$ ,  $T_N^X$ , or  $\beta_X$  depending on the dictionary

As an example,

```
coef_dict = {'bcc': {'Al' : {0: -438, 1: 1720, 'pureX' : 0}, 'C':...}, 'fcc':...}
```

The coefficients in this version of the code are predominantly for the  $\alpha$ -BCC phase of Fe alloys, and the details of their calculation can be found in Murdoch et al.<sup>13</sup> Coefficients for the  $\gamma$  and  $\epsilon$  phases are still in development and not included in this version of the functions.

```
alloy_curiel_neel(mol_comp_dict, phase = 'bcc', calc_type='EXT', temp_type='Curie', feTc = 1043):
```

### Purpose

- Calculate either Curie or Néel temperature as a function of alloy content given coefficients for polynomial fit
- Currently uses BINARY parameters only, no ternary or higher higher-order interactions

### Parameters

- mol\_comp\_dict: dictionary of compositions in atomic fraction
- phase: the phase of interest, used as the one of the keys in the coefficient dictionary. The default is ‘bcc.’
- calc\_type: chooses the coefficient dictionary to use
  - ‘EXT’ for calculating external field magnetization/energy,
  - ‘INT’ for calculating the internal magnetic free energy (effective).
  - The default is ‘EXT.’
- temp\_type: magnetic transition temperature type Curie/Néel. The default is ‘Curie.’
- feTc: Curie temperature of iron. can be changed if doing Néel or paramagnetic Curie. The default is 1043.

### Returns

- alloy: Curie/Néel temperature at composition X

*alloy\_moment(mol\_comp\_dict, phase='bcc', calc\_type = 'EXT', mFe = 2.22):*

### Purpose:

- Calculate AVG moment as a function of alloy content given coefficients for polynomial fit
- Currently uses BINARY parameters only, no ternary or higher higher-order interactions

### Parameters

- mol\_comp\_dict: dictionary of composition in ATOMIC FRACTION
- phase: the phase of interest, used as the one of the keys in the coefficient dictionary. The default is ‘bcc.’
- calc\_type: chooses the coefficient dictionary to use

- ‘EXT’ for calculating external field magnetization/energy,
- ‘INT’ for calculating the internal magnetic free energy (effective).
- The default is ‘EXT.’
- mFe: moment of iron. The default is 2.22.

Returns

- alloy: the magnetic moment of the alloy in  $\mu\text{B}$

*neel\_gamma\_empirical(elemsAT):*

Purpose:

- Empirical equation for Néel temperature of the GAMMA phase given composition (Aristeidakis and Haidemenopoulos<sup>29</sup>).

Parameters

- elemsAT: dictionary of composition in atomic fraction

Returns

- $T_N$ : Néel temperature in Kelvin

*neel\_epsilon\_empirical(elemsAT):*

Purpose:

- Empirical equation for Néel temperature of the EPSILON phase given composition (Aristeidakis and Haidemenopoulos<sup>29</sup>).

Parameters

- elemsAT: dictionary of composition in atomic fraction

Returns

- $T_N$ : Néel temperature in Kelvin

These functions are used to build the magnetic property dictionaries associated with the **steel\_class**. The dictionaries in the class have the following format:

{‘phase’: {‘m’: value, ‘Tc’: value, ‘Tn’: value, ‘Neelfactor’: value}}}

Units of the magnetic moment,  $m$ , are Bohr magneton,  $\mu\text{B}$ . The value for pure Fe would be 2.22, as in 2.22  $\mu\text{B}$ . The units of the magnetic transition temperature are Kelvin. The required and optional magnetic property dictionary keys are in Table 3.

**Table 3 Keys in magnetic property dictionaries**

Key	Property	Units
m	Magnetic moment	$\mu_B$
Tc	Curie temperature	K
theta	Paramagnetic Curie temperature	K
Tn	Néel temperature	K
Neelfactor	Ratio of $\theta / T_N$	...

An optional key is ‘Neelfactor,’ which is the constant that describes the relationship between the  $T_N$  and the transition temperature  $\theta$  in the susceptibility Eq. 6, as described in Section 1.1.2.2. This factor is a function of crystal structure and antiferromagnetic type. The key ‘theta’ is also optional as the paramagnetic  $T_c$  would be preferred for use in calculating the paramagnetic susceptibility.

Note that many functions associated with the  $\gamma$  and  $\epsilon$  phases will be making decisions about the antiferromagnetic state based on whether the magnetic coefficient dictionary contains the key ‘Tn’ for a  $T_N$ . Therefore, if the material does not have a  $T_N$ , do not include it as a key with an empty value.

There are three magnetic property dictionaries contained in the `steel_class` and used in the various magnetic functions:

- *mag\_prop*: the values calculated by user for use in magnetization and susceptibility calculations and the IHJ form of the internal magnetic energy
- *effective\_mag\_prop*: the values calculated by user for use in Xiong internal magnetic energy calculation
- *calphad\_mag\_prop*: the values contained in the CALPHAD database (e.g., Thermo-Calc TCFE10). These may be necessary to calculate the replacement of the IHJ internal magnetic energy with the Xiong internal magnetic energy depending on how the total free energies are assessed.

The *mag\_prop* dictionary would be calculated using the ‘EXT’ calculation type in the alloy property functions, and *effective\_mag\_prop* dictionary would be calculated using the ‘INT’ calculation type.

## **2.3 Functions for Free Energy of a Phase**

---

The overarching function *magnetic\_energies()* calls the function to get the total free energy of the phases from Thermo-Calc and the functions to calculate the magnetic contribution to the free energy for each individual phase. If you are not using Thermo-Calc you would omit this function and just call the functions for the magnetic contribution of the individual phases directly.

*magnetic\_energies(field, steel, path):*

Purpose:

- Calculates contribution of magnetic field to free energy of alpha phase
- Uses: `alpha_gamma_epsilon_energy()` – requires ThermoCalc `magnet_alpha()`, `magnet_gamma()`, `magnet_epsilon()`

Parameters

- `field`: applied magnetic field in Tesla
- `steel`: instance of the class that includes name, composition, and magnetic properties

Returns

- Results: dataframe including free energies of alpha and gamma phases at 0T and {field}T, also exported to comma-separated value (CSV) file

### 2.3.1 CALPHAD Free-Energy Functions

These functions require Thermo-Calc and the TC-Python Application Programming Interface (API) in their current format. In this function, the IHJ internal energy is swapped for the Xiong internal energy, necessitating the use of the *effective\_magnet\_prop* dictionary.

*alpha\_gamma\_epsilon\_energy(steel, filepath, tmax = 1000, tmin = 0.1, tstep = 0.1)*

Purpose:

- Function to get free energies of alpha (BCC\_A2), gamma (FCC\_A1), and epsilon (HCP\_A3) phases from Thermo-Calc
- Also returns the T<sub>c</sub> and moment as a function of alloy content as defined by the Thermo-Calc database coefficients (not the coefficients we have defined using the alloy functions)

Parameters

- `composition`: dictionary of alloy in WEIGHT PERCENT
- `name`: name of the alloy for logfile and results file

Returns

- `totalresult`: dataframe of temperature (index), G(bcc), G(fcc)

- `thermocalc_magnet_prop`: dictionary of Curie temp and moment for the phases

### 2.3.2 Calculations for the Individual Phases

The choice for what magnetic state a given phase is in is contained within the `magnet_{phase}()` functions, but the general decision-making tree is illustrated in Fig. 6.

#### 2.3.2.1 $\alpha$ Phase

The `magnet_alpha()` function returns a dataframe with temperature as the index and the various columns of magnetic contributions; for the external contribution it is one column where the values will be from the ferromagnetic description up until  $T_c + 40$  K and then paramagnetic description thereafter.

Within `magnet_alpha()`, the temperature is checked against the  $T_c$  to determine whether to use ferromagnetic or paramagnetic description. The  $T_c$  is calculated from `new_TC_from_field()`. The criteria,  $T_c + 40$  K, is determined from experimental observations in pure Fe (i.e., the Curie–Weiss form of the paramagnetic description [Eq. 5] only begins to be valid at a certain point above the Curie temperature<sup>30</sup>). As an example, we see for pure Fe the magnetization under an applied field of 10 Tesla with two experimental data points by Hao and Ohtsuka<sup>1</sup> in Fig. 7; the solid red curve is the magnetization calculated by Kuz'min ferromagnetic theory and the dashed curve is the magnetization by the Curie–Weiss paramagnetic description. The asymptote for the magnetization for the paramagnetic region under applied field is what we are avoiding with the  $T_c + 40$  K criteria.

```
magnet_alpha(field, temperaturearray, steel, nofieldarray = np.linspace(1e-5, 1, 100001), magarray = np.linspace(1e-5, 1.01, 100001)):
```

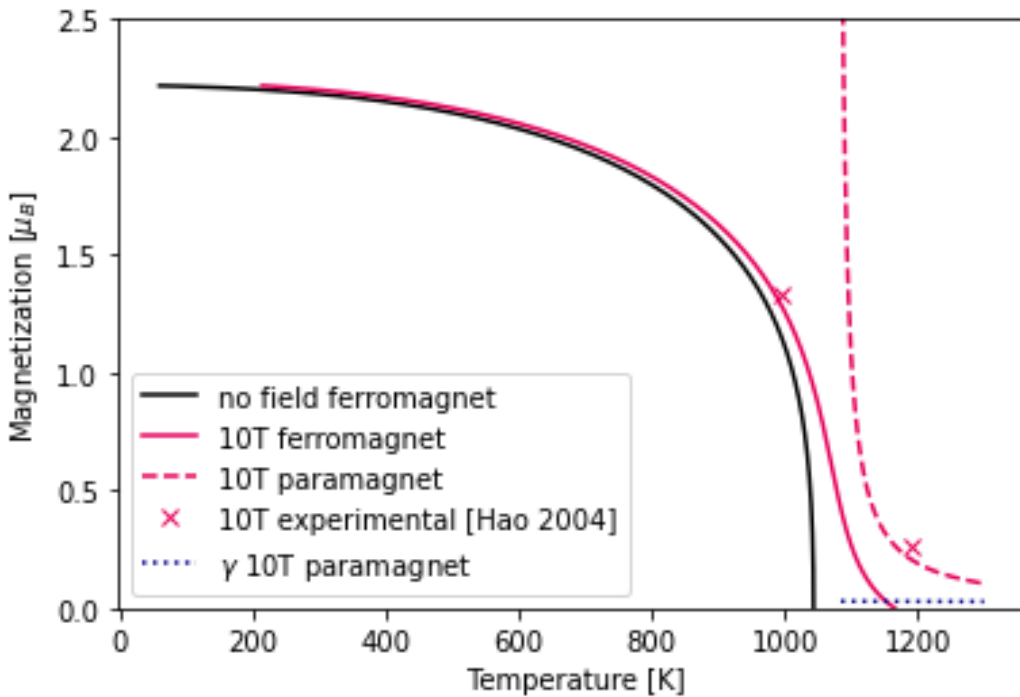


**Fig. 7 Diagram of ferromagnetic and paramagnetic models for  $\alpha$  phase; experimental magnetization points at 10 Tesla are from Hao and Ohtsuka<sup>1</sup>**

#### Purpose:

- Calculates contribution of applied magnetic field to ALPHA phase
- Uses: `landau()` for ferromagnetic and `dG_para()` if paramagnetic, `dG_INTERNAL_ferromagnet()` for both

#### Parameters

- `field`: applied field in Tesla
- `temperaturearray`: array of temperature
- `steel`: instance of the steel class that includes the magnetic properties
- `nofieldarray`: array of reduced magnetization (`sigma`) to solve Landau description for ferromagnet, no field
  - The default is `np.linspace(1e-5,1,100001)`.
- `magarray`: array of reduced magnetization (`sigma`) to solve Landau description for ferromagnet, no field
  - The default is `np.linspace(1e-5,1.01,100001)`.

## Returns

- fieldresults\_alpha: dataframe with index of temperature, columns of change to free energy and magnetization due to applied field

### 2.3.2.2 $\gamma$ Phase

The function *magnet\_gamma()* checks for a  $T_N$  in the magnetic properties of the instance of the steel class. If it is present in **steel\_class.mag\_prop**, it will treat the phase as antiferromagnetic and use the associated functions; if not, it will use the paramagnetic functions.

*magnet\_gamma(field, temperaturearray, steel):*

#### Purpose:

- Calculates contribution of applied magnetic field to GAMMA phase
- Checks for antiferromagnetic phase
- Uses: dG\_INTERNAL\_ferromagnet() and dG\_fcc\_para() if paramagnetic,
  - dG\_INTERNAL\_AFM and dG\_AFM\_paramagnetic() if antiferromagnetic

#### Parameters

- field: magnetic field strength in Tesla
- temperaturearray: list of temperatures to do free energy calculation at
- steel: instance of the steel class that includes the magnetic properties

## Returns

- fieldresults\_epsilon: dataframe with index of temperature, columns of change to free energy due to applied field

### 2.3.2.3 $\epsilon$ Phase

The function *magnet\_epsilon()* checks for a  $T_N$  in the magnetic properties of the instance of the steel class. If it is present in **steel\_class.mag\_prop**, it will treat the phase as antiferromagnetic and use the associated functions; if not, it will use the paramagnetic functions.

*magnet\_epsilon(field, temperaturearray, steel):*

#### Purpose:

- Calculates contribution of applied magnetic field to EPSILON phase

- Checks for antiferromagnetic phase
- Uses: `dG_INTERNAL_ferromagnet()` if paramagnetic,  
`dG_INTERNAL_AFMs` and `dG_AFMs_paramagnetic()` if antiferromagnetic

#### Parameters

- field: magnetic field strength in Tesla
- temperaturearray: list of temperatures to do free energy calculation at
- steel: instance of the steel class that includes the magnetic properties

#### Returns

- `fieldresults_epsilon`: dataframe with index of temperature, columns of change to free energy due to applied field

## **2.4 Functions for Internal Magnetic Energy Change**

---

There are two main functions for calculating the term  $G_{internal}^{magnetic}$  as part of the phase description:

- `dG_INTERNAL_ferromagnet()`: for phases with a ferromagnetic state, which uses the  $T_c$  for the reduced temperature,  $\tau$ , and calculates the shift in  $T_c$  under an applied field with the function `new_TC_from_field()`.
- `dG_INTERNAL_AFMs`: for phases with an antiferromagnetic state, which uses the  $T_N$  for the reduced temperature,  $\tau$ , and currently assumes no change to the  $T_N$  under an applied field. As no change to the transition temperature will result from an applied field, this calculation performed by this function will currently result in a change of 0 J/mol to the internal energy. However, in the future, texture effects may want to be accounted for, which could shift the  $T_N$  under applied field in measurable ways.

The other functions used in calculating the internal magnetic energy refer to the equations of Section 1.3.1 and the switch from the IHJ model to the Xiong model. The function `g_internal_swap()` in particular calculates the difference in the predicted internal magnetic energy by the IHJ model versus the Xiong model.

`dG_INTERNAL_ferromagnet(field, effective_magnet_prop,  
temperature_array, structure = 'bcc'):`

#### Purpose:

- Calculate internal magnetic energy in no field and field

- Uses change in Curie temperature with applied field, `new_TC_from_field()`
- and functions `g_tau_IHJ()` and `g_tau_xiong()` for internal entropy calculation

#### Parameters

- field: applied field in [Tesla]
- Tc: curie temperature of alloy in [K]
- m: magnetic moment of alloy in [uB], (e.g., 2.2 uB)
- temperature\_array: temperature list to iterate through, from dataframe of free energy values in [K]
- structure = phase bcc/fcc/hcp, needed for G functions

#### Returns

- dGinternal: list of difference between internal magnetic energy IN FIELD and without in [J/mol]

#### Uses/Needs

- `new_TC_from_field()`
- `g_tau_xiong()`

`dG_INTERNAL_AFM(field, effective_magnet_prop, temperature_array, structure = 'bcc'):`

#### Purpose

- Calculate internal magnetic energy in no field and field
- and functions `g_tau_xiong()` for internal entropy calculation

#### Parameters

- Field: applied field in [Tesla]
- TN: Neel temperature of alloy in [K]
- m: magnetic moment of alloy in [uB], (e.g., 2.2 uB)
- temperature\_array: temperature list to iterate through, from dataframe of free energy values in [K]
- structure = phase bcc/fcc/hcp, needed for G functions

## Returns

- dGinternal: list of difference between internal magnetic energy IN FIELD and without in [J/mol]

## Uses / Needs

- g\_tau\_xiong()

*g\_internal\_swap(temperature\_array, thermocalc\_magnet\_prop,  
effective\_magnet\_prop, structure = 'bcc'):*

## Purpose

- Function to replace the internal magnetic energy calculated in CALPHAD using IHJ model
- with internal magnetic energy calculated via Xiong model
- Uses: g\_tau\_IHJ() , g\_tau\_xiong()

## Parameters

- temperature\_array: temperature list to iterate through, from dataframe of free energy values in [K]
- thermocalc\_magnet\_prop: dictionary of the magnetic properties from CALPHAD database
- effective\_magnet\_prop: dictionary of effective magnetic properties after the Xiong model
- structure: crystal structure of the phase. The default is bcc.

## Returns

- GintIHJ: internal magnetic energy using the IHJ model
- Gint\_xiong: internal magnetic energy using the Xiong model.

*g\_tau\_IHJ(tau, structure='bcc'):*

## Purpose

- IHJ function for internal magnetic ordering
- $G_{mag\_internal} = R * T * \text{np.log}(\beta + 1) * g_{tau}$

## Parameters

- tau: temperature/Tc

- structure: used for structure factor, p; default is bcc

Returns

- gtau: value of IHJ function at that temperature

*g\_tau\_xiong(tau, structure='bcc'):*

Purpose:

- Xiong function for internal magnetic ordering  
[<https://doi.org/10.1016/j.calphad.2012.07.002>]  
 $G_{mag\_internal} = R * T * \text{np.log}(\beta * + 1) * g_{\tau}$

Parameters

- tau: reduced temperature,  $T/T_c$  or  $T/T_N$
- structure: crystal structure of the phase. The default is bcc.

Raises

- AttributeError: if incorrect structure/phase is entered

Returns

- gtau: value of function  $g_{\tau}$ .

## 2.5 Functions for External Magnetic Energy Change

---

### 2.5.1 Ferromagnetic State

There is no standalone function for the free-energy change when the phase is in the ferromagnetic state, as it is more computationally efficient (given that the magnetization must be numerically solved) to calculate all at once in the *magnet\_alpha()* function.

### 2.5.2 Paramagnetic State

The following functions describe the various possible paramagnetic states:

- *dG\_para()*: paramagnetic state of a phase with a  $T_c$  (e.g., for calculations at temperatures above the paramagnetic  $T_c$ )
- *dG\_AFM\_paramagnetic()*: paramagnetic state of a phase with a  $T_N$  (e.g., for calculations at temperatures above the  $T_N$ )
- *dG\_fcc\_para()*: paramagnetic  $\gamma$  phase (e.g., does not have a  $T_N$ /antiferromagnetic state). Currently using the susceptibility equation of

pure Fe from Gao et al.<sup>12</sup> Since the contribution in the phase/magnetic state is very small compared to other possibilities, this function does not take a variation as a function of alloy content.

Recall from Eq. 20 the external energy term in a paramagnetic state is

$$G_{paramagnetic}^{external} = \frac{1}{2}\mu_0\chi H^2$$

The final units for the free energy need to be in J/mol. The starting units of the applied field input are Tesla, and the susceptibility,  $\chi$ , units from the *para\_susceptibility()* and *AFM\_susceptibility()* functions are cm<sup>3</sup>/g. The applied field is converted from Tesla to A/m:  $1[T] = 7.958 \times 10^5 \left[ \frac{A}{m} \right]$

The units for the rest of the Eq. 20 follow, including incorporation of molar mass (which is input as g/mol):

$$\frac{1}{2}\mu_0 \left[ \frac{Wb}{A \cdot m} \right] \chi^\gamma \left[ \frac{cm^3}{g} \right] H^2 \left[ \frac{A}{m} \right]^2 \quad (21a)$$

$$Wb = \left[ \frac{J}{A} \right] \text{ and } \left[ \frac{cm^3}{g} \right] = 4\pi \times 10^{-3} \left[ \frac{m^3}{kg} \right] \quad (21b)$$

$$\frac{1}{2}\mu_0 \left[ \frac{J}{A^2 \cdot m} \right] \chi^\gamma 4\pi \times 10^{-3} \left[ \frac{m^3}{kg} \right] H^2 \left[ \frac{A}{m} \right]^2 \quad (21c)$$

$$\frac{1}{2}\mu_0 \left[ \frac{J}{A^2 \cdot m} \right] \chi^\gamma 4\pi \times 10^{-3} \left[ \frac{m^3}{kg} \right] H^2 \left[ \frac{A}{m} \right]^2 \frac{M}{1000} \left[ \frac{kg}{mol} \right] \quad (21d)$$

*dG\_para(T, our\_magnet\_prop, molar\_mass, magstrength, j = 1):*

### Purpose

- Calculates free energy of paramagnetic alpha (BCC) phase under applied magnetic field
- Returns one value at one temperature point
- Parameters
- T: temperature
- our\_magnet\_prop: dictionary of magnetic properties
- magstrength: applied field in Tesla
- j: WMFT parameter, = 1 for paramagnetic

### Returns

- dG: change in free energy from magnet in J/mol

*dG\_AFM\_paramagnetic(T, our\_magnet\_prop, molar\_mass, magstrength, structure = 'bcc'):*

### Purpose:

- Calculates free energy of antiferromagnetic phase above  $T_N$  under applied magnetic field
- Returns one value at one temperature point

### Parameters

- T: temperature
- our\_magnet\_prop: dictionary of magnetic properties
- molar\_mass: molar mass of alloy
- magstrength: field strength in Tesla
- structure: crystal structure of phase. The default is bcc.

### Returns

- dG\_afm: change in free energy from magnet in J/mol

*dG\_fcc\_para(T, magstrength, molar\_mass):*

### Purpose:

- Calculates free energy of paramagnetic fcc phase under applied magnetic field
- No alloy change – this is pure Fe
- [Gao et al.<sup>12</sup>; <https://doi.org/10.1088/0022-3727/39/14/003>]

### Parameters

- T: temperature
- magstrength: applied field in Tesla
- molar\_mass: molar mass of alloy

### Returns

- dGfcc: change in free energy from magnet in J/mol

## 2.6 Functions for Magnetic States

---

### 2.6.1 Ferromagnetic State

The primary function for ferromagnetic calculations is *landau()*, which calculates the magnetization curve of an alloy. It is possible to solve the Kuz'min–Landau equations for a single magnetization at a given temperature; however, it is far more efficient to feed the Landau model a very finely spaced array of reduced magnetizations ( $M/M_0$  will be from 0 to 1) and then locate the temperature of interest in the solution array. Under an applied field, the magnetization array will need to be slightly larger (e.g., 0 to 1.05), so functions that call *landau()*, such as *magnetization\_curves()*, will generally have two arguments with default arrays for field and no field cases.

As discussed in Section 1.3.1, the  $T_C$  of an alloy will increase under an applied field. This is calculated via *new\_TC\_from\_field()*, which uses the inflection point of the magnetization curve to determine the new  $T_C$  under the given field.

*landau(H, sig, Tc=1043, m0=2.22, p=0.25, k=0.18, a0=3.3)*

Purpose:

- Calculate magnetization of an alloy using Kuz'min application of Landau<sup>9</sup>

Parameters

- H: applied field in Tesla
- sig: array of reduced magnetization ( $M/M_0$ )
- Tc:  $T_C$  of the alloy in [K]. The default is 1043.
- m0: magnetic moment of the alloy in [ $\mu_B$ ]. The default is 2.22.
- p: coefficient in model. The default is 0.25 (pure Fe).
- k: coefficient in model. The default is 0.18 (pure Fe).
- a0: coefficient in model. The default is 3.33 (pure Fe).

Returns

- [T, m]: array of temperature [K] and magnetization [ $\mu_B$ ] values

*magnetization\_curves(TCalloy, malloy, field, magarray=np.linspace(1e-5, 1.01, 1001), nofieldarray=np.linspace(1e-5, 1.0, 1001)):*

Purpose:

- Calculates magnetization curves for no field and applied field for a given alloy

#### Parameters

- TCalloy: Tc of the alloy
- malloy: magnetic moment of the alloy
- field: applied magnetic field in Tesla
- magarray: array of reduced magnetization values for field-induced magnetization. The default is np.linspace(1e-5,1.01,1001).
- nofieldarray: array of reduced magnetization values for no field magnetization. The default is np.linspace(1e-5,1.01,1001).

#### Returns

- field\_magnetization: array of [T, M] under applied field
- nofield\_magnetization: array of [T, M] for zero field

*new\_TC\_from\_field(field, Tc, m0):*

#### Purpose

- Function to calculate shift in Tc under applied field

#### Parameters

- field: applied field in [Tesla]
- Tc: Curie temperature of alloy in [K]
- m0: magnetic moment of alloy in [uB]

#### Returns

- newTC: Curie temperature under applied field in [K]

#### Uses

- *landau(H, sig, Tc=1043, m0=2.22, X=0., p=0.25, k=0.18, a0=3.3)*

### 2.6.2 Functions for Paramagnetic State

#### 2.6.2.1 Susceptibility of Phase above Curie Temperature

The susceptibility is calculated with the function *para\_susceptibility()*;  $\mu_B$ .

The derivation of these equations is detailed in the following, including units' conversions for reference.

$$\chi = \mu_0 \frac{N_{AV}}{M} \frac{(j+1)}{3j} \frac{\{\beta_{alloy}\}^2}{k(T-\theta_{alloy})} \left( \frac{1000}{4\pi \times 10^{-3}} \right) \left[ \frac{cm^3}{g} \right] \quad (22)$$

where M is molar mass in [g/mol],  $N_{AV}$  is Avogadro's number, and  $j$  is the WMFT parameter, which is 1 for paramagnetic materials.

*para\_susceptibility(T, malloy, thetaalloy, j = 1):*

#### Purpose:

- Calculates paramagnetic susceptibility using alloy form of Curie–Weiss
- Murdoch et al. 2021a<sup>10</sup>

#### Parameters

- $T$ : temperature in Kelvin
- $malloy$ : magnetic moment of the alloy in  $\mu_B$
- $thetaalloy$ : paramagnetic curie temperature of the alloy, in Kelvin
- $j$ : WMFT parameter, = 1 for paramagnetic

#### Returns

- susceptibility: susceptibility at a given temperature [cm<sup>3</sup>/g]

The change to the free energy as a consequence of an applied field using this susceptibility is the function *dG\_para()*.

#### 2.6.2.2 Susceptibility of Phase above Néel Temperature

$$\chi = \mu_0 \frac{N_{AV}}{3Mk} \frac{\{\beta_{alloy}\}^2}{(T-\theta)} \left( \frac{1000}{4\pi \times 10^{-3}} \right) \left[ \frac{cm^3}{g} \right] \quad (23)$$

where M is molar mass in [g/mol].

*AFM\_susceptibility(T, malloy, neel, neelfactor = -1):*

#### Purpose:

- calculates susceptibility for antiferromagnetic phase

#### Parameters

- $T$ : temperature in Kelvin

- *malloy*: magnetic moment in  $\mu\text{B}$
- *neel*:  $T_N$
- *neelfactor*:  $\theta_{AF}$  is a function of the crystal structure and is neelfactor \* Néel. The default is -1.

Returns

- susceptibility: antiferromagnetic susceptibility at a temperature [ $\text{cm}^3/\text{g}$ ]

### 2.6.2.3 Susceptibility of Phase without Curie/Néel Temperature

For a paramagnetic material (e.g., the  $\gamma$  phase in pure Fe<sup>12</sup>):

$$\chi^\gamma = \frac{1.33 \times 10^{-1}}{T + 3451} \left[ \frac{\text{cm}^3}{\text{g}} \right] \quad (24)$$

*gamma\_susceptibility(T)*:

Purpose

- Calculates susceptibility of gamma phase using Gao<sup>12</sup>

Parameters

- $T$ : temperature in Kelvin

Returns

- susceptibility: susceptibility in  $\text{cm}^3/\text{g}$

### 2.6.3 Functions for Antiferromagnetic State

At this time, we are not considering the effect of magnetic field on the antiferromagnetic state of the  $\gamma$  or  $\epsilon$  phase due to the complexities that arise from orientation dependence and the fact that the  $T_N$  is often lower than room temperature and not a traditionally viable processing space.

*AFM()*:

Purpose:

Placeholder function if we ever want to describe below the  $T_N$

Returns

- 0; in the future would return susceptibility at temperature

## 2.7 Martensite Transformation Functions

---

There are two martensite transformations considered in this code,  $\gamma \rightarrow \alpha$ -martensite and  $\gamma \rightarrow \epsilon$  martensite. Each transformation has a parent function *transformation\_gamma\_alpha()* or *transformation\_gamma\_epsilon()*, respectively. Each transformation has a driving force; in the case of the  $\gamma \rightarrow \alpha$ , this driving force is calculated using the Stormvinter model<sup>31</sup> with the coefficients modified to account for the Xiong internal energy model instead of the original IHJ model. For the  $\gamma \rightarrow \epsilon$ , the driving force model is based on the stacking fault energy (SFE) as described in Lloyd et al.<sup>32</sup> and Pisarik and Van Aken.<sup>33</sup>

### 2.7.1 $\gamma \rightarrow \alpha$ -martensite

*transformation\_gamma\_alpha(results, field, composition, name):*

#### Purpose

- calculate the alpha martensite start temperature under applied field

#### Parameters

- results: dataframe of results from free energy calculation
- field: applied field in Tesla
- composition: composition dictionary for alloy
- name: name of alloy (for plot title...)

#### Returns

- nomag\_Ms: martensite start temperature for 0 applied field
- fullmag\_Ms: martensite start temperature for applied field including both internal and external contributions
- extmag\_Ms: martensite start temperature for applied field including external contributions ONLY

*stormvinter\_lathIII\_effective(composition):*

#### Purpose:

- Driving force for alpha martensite lath using Stromvinter model<sup>31</sup>
- Coefficients have been refit to account for effective thermodynamic properties/Xiong internal energy model

#### Parameters

- composition: dictionary of composition (in AT PERCENT)

Returns

- Driving force in J/mol

*stormvinter\_plateIV\_effective(composition):*

Purpose:

- Driving force for alpha martensite plate using Stromvinter model
- Coefficients have been refit to account for effective thermodynamic properties/Xiong internal energy model

Parameters

- composition: dictionary of composition (in AT PERCENT)

Returns

- Driving force in J/mol

## 2.7.2 $\gamma \rightarrow \epsilon$ -martensite

The  $\epsilon$ -martensite driving force can be estimated via the stacking fault energy (see Lloyd et al.<sup>32</sup> and Pisarik and Van Aken<sup>33</sup>). As the coefficient dictionary for the  $\epsilon$  phase is not yet complete, this function is not currently included in the code module.

## 3. Examples

---

The example script, MAGNETS\_examples.ipynb, which is in Appendix B, contains the following sections:

- “Comparison of Susceptibility Fit to Data”
- “Example Magnetization Curve”
- “Free Energy Examples”

These are described in the following. A fourth example, that of the  $\gamma \rightarrow \alpha$ -martensite transformation, is described in Section 3.3 but does not have an accompanying example script as it requires the Thermo-Calc software to run.

### 3.1 Magnetization Curve and Susceptibility of Some Alloys

---

The code section “Comparison of Susceptibility Fit to Data” compares the susceptibility calculated by the empirical fits for the Fe-V system<sup>13</sup> and the function

*para\_susceptibility()* to the measured susceptibility of Arajs et al.<sup>34</sup> The results are in Fig. 8, with the experimental measurements as points and the fit as lines. The fit is quite good up to a fairly high amount of V content, and the expected trend of an increase in inverse susceptibility with increasing alloy content is captured well.

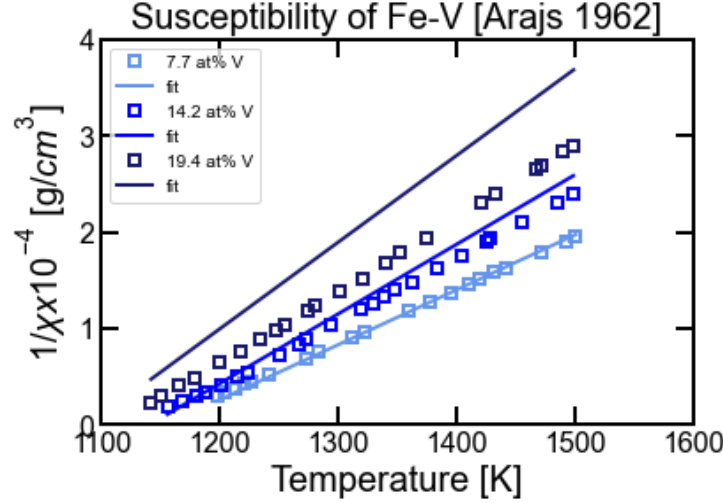


**Fig. 8** Plot of predicted susceptibility for the paramagnetic state of Fe-V. Experimental data as points from Arajs et al.<sup>34</sup> and fit as lines from the *para\_susceptibility()* function.

The code section “Example Magnetization Curve” shows the calculation of the magnetization for the ferromagnetic state for no field and for an applied field of 20 Tesla using the function *magnetization\_curves()*. The curves are shown in Fig. 9.

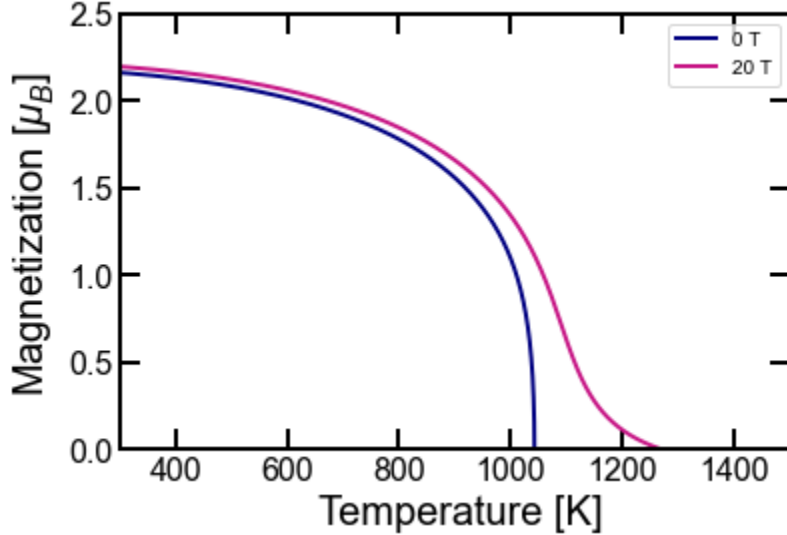


**Fig. 9** Example plot of magnetization curves at no field (navy) and an applied field of 20 Tesla (pink) using the *magnetization\_curves()* function

### 3.2 Free-Energy Curves

---

The code section “Free Energy Examples” sets up the magnetic property dictionaries for a given example alloy and then calculates the change in free energy under an applied field for the three phases. In this example, the  $\gamma$  and  $\epsilon$  phases are antiferromagnetic, and the energy change is calculated for the paramagnetic state. The free-energy change for an example ferromagnetic state is in Fig. 10. The example free-energy changes for the paramagnetic state are in Fig. 11.

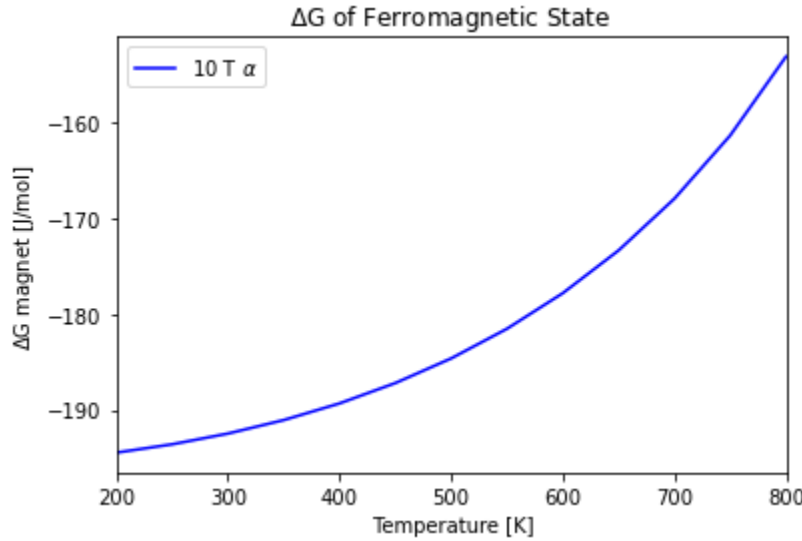


**Fig. 10** Plot of free-energy change from an applied field of 10 Tesla for the ferromagnetic  $\alpha$  phase

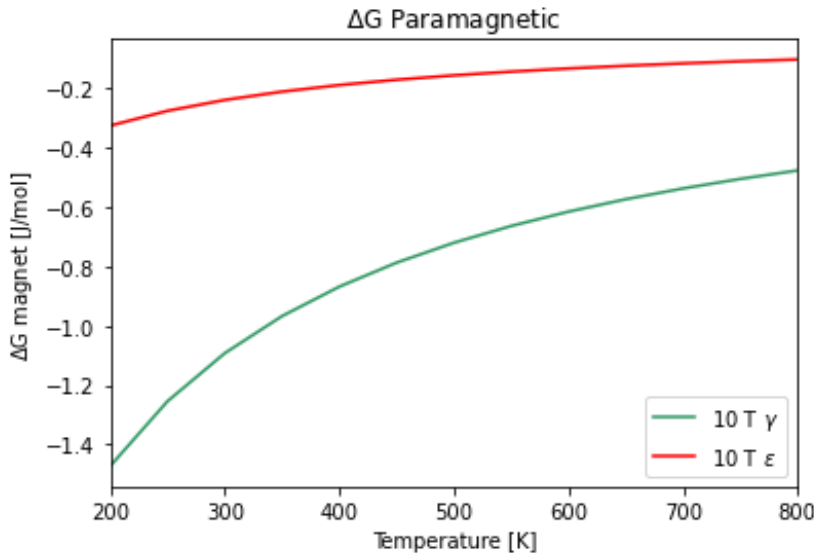


**Fig. 11** Plot of free-energy change from an applied field of 10 Tesla for the paramagnetic state of the antiferromagnetic  $\gamma$  and  $\epsilon$  phases

### 3.3 Martensite Transformation

---

Because an example of the martensite transformation calculation under an applied field requires the Thermo-Calc Python API,<sup>35</sup> we do not include a script example, but an example output is shown in Fig. 12. This is the shift in the martensite start (Ms) temperature for the lath and plate forms of martensite under an applied field of 10 Tesla. The points are experimentally observed Ms for Fe-Mn alloys.<sup>31</sup> The Thermo-Calc database used is TCFE10.<sup>36</sup>

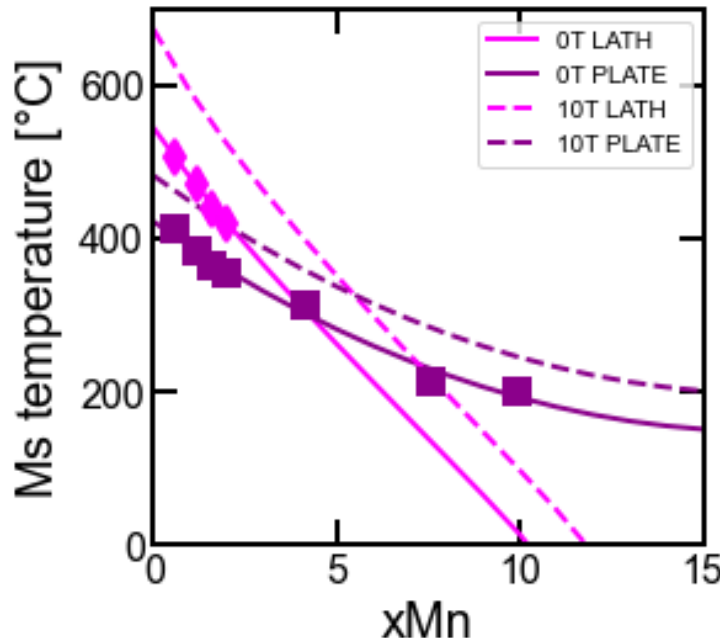


Fig. 12 Plot of shift in Ms temperature for both lath and plate forms from no field to an applied field of 10 Tesla for Fe-Mn alloys. Points are experimental observations from Stormvinter,<sup>31</sup> and lines are the predicted Ms values from the *transformation\_gamma\_alpha()* function.

## 4. Conclusions and Future Work

---

The *MAGNETS.py* module enables calculation of the magnetization for paramagnetic and ferromagnetic states of Fe-based alloys through the use of empirical fit dictionaries and theoretical functions. The magnetization can then be used to calculate the change to the free energy of a phase through another series of functions, including contributions to both the internal free energy of the phase and an additional term for the external field contribution. An example script highlights the possible magnitude of changes to the free energy due to an applied field and concludes with an example of those changes influencing the Ms temperature.

A comprehensive dictionary for the  $\alpha$ -ferrite phase in Fe-based alloys is included with this module, while the dictionaries for the  $\gamma$  and  $\epsilon$  phases are still in development. Further, while the paramagnetic state of an antiferromagnet (e.g., above the  $T_N$ ) is currently well described in the code, the antiferromagnetic state is not.

## 5. References

---

---

1. Hao XJ, Ohtsuka H. Effect of high magnetic field on phase transformation temperature in Fe-C alloys. *Materials Transactions*. 2004;45(8):2622–2625.
2. Rivoirard S, Garcin T, Gaucherand F, Bouaziz O, Beaugnon E. Dilatation measurements for the study of the  $\alpha/\gamma$  transformation in pure iron in high magnetic fields. *Journal of Physics: Conference Series*. 2006 November;51(1):122. IOP Publishing.
3. Mitsui Y, Ikehara Y, Takahashi K, Kimura S, Miyamoto G, Furuhara T, Koyama K. Fe-Feinf3infC binary phase diagram in high magnetic fields. *Journal of Alloys and Compounds*. 2015;632:251–255.
4. Garcin T, Rivoirard S, Beaugnon E. Thermodynamic analysis using experimental magnetization data of the austenite/ferrite phase transformation in Fe–xNi alloys ( $x = 0, 2, 4$  wt%) in a strong magnetic field. *Journal of Physics D: Applied Physics*. 2010;44(1):015001.
5. Fukuda T, Yuge M, Lee JH, Terai T, Kakeshita T. Effect of magnetic field on  $\gamma$ – $\alpha$  transformation temperature in Fe-Co alloys. *ISIJ International*. 2006;46(9):1267–1270.
6. Shimizu KI, Kakeshita T. Effect of magnetic fields on martensitic transformations in ferrous alloys and steels. *ISIJ International*. 1989;29(2):97–116.
7. Hou TP, Peet MJ, Hulme-Smith CN, Wu KM, Li Y, Guo L. The determining role of magnetic field in iron and alloy carbide precipitation behaviors under the external field. *Scripta Materialia*. 2016;120:76–79.
8. Hou TP, Li Y, Wu KM, Peet MJ, Hulme-Smith CN, Guo L. Magnetic-field-induced magnetism and thermal stability of carbides  $Fe_{6-x}Mo_xC$  in molybdenum-containing steels. *Acta Materialia*. 2016;102:24–31.
9. Kuz'min M. Landau-type parametrization of the equation of state of a ferromagnet. *Physical Review B*. 2008;77(18):184431.
10. Murdoch HA, Hernández-Rivera E, Giri A. Modeling magnetically influenced phase transformations in alloys. *Metallurgical and Materials Transactions A*. 2021a;52(7):2896–2908.
11. Crangle J, Goodman G. The magnetization of pure iron and nickel. *Proc R Soc London, Ser A*. 1971;321(1547):477–491.

12. Gao MC, Bennett TA, Rollett AD, Laughlin DE. The effects of applied magnetic fields on the  $\alpha/\gamma$  phase boundary in the Fe-Si system. *Journal of Physics D: Applied Physics.* 2006;39(14):2890. doi.org/10.1088/0022-3727/39/14/003.
13. Murdoch H, Giri A, Field D, Hernández-Rivera E, Guziewski M. Magnetically altered phase stability in Fe-based alloys: modeling and database development. *Calphad.* 2021b;75:102360.
14. Bigdeli S, Selleby M. A thermodynamic assessment of the binary Fe-Mn system for the third generation of Calphad databases. *Calphad.* 2019;64:185–195.
15. Xiong W, Selleby M, Chen Q, Odqvist J, Du Y. Phase equilibria and thermodynamic properties in the Fe-Cr system. *Critical Reviews in Solid State and Materials Sciences.* 2010;35(2):125–152.
16. Ohnuma I, Enoki H, Ikeda O, Kainuma R, Ohtani H, Sundman B, Ishida K. Phase equilibria in the Fe-Co binary system. *Acta Materialia.* 2002;50(2):379–393.
17. Korn J. The influence of an external magnetic field on the magnetic part of the specific heat of a ferromagnetic substance. *Journal of Materials Science.* 1970;5(5):407–410.
18. Connelly DL, Loomis JS, Mapother DE. Specific heat of nickel near the Curie temperature. *Physical Review B.* 1971;3(3):924.
19. Gschneidner KA Jr, Pecharsky VK. The influence of magnetic field on the thermal properties of solids. *Materials Science and Engineering: A.* 2000;287(2):301–310.
20. Chui CP, Zhou Y. Investigating the magnetovolume effect in isotropic body-centered-cubic iron using spin-lattice dynamics simulations. *AIP Advances.* 2014;4:087123. doi.org/10.1063/1.4893469.
21. Morrish AH. *The physical principles of magnetism.* Wiley; 1965.
22. Boersma F, Cooper DM, de Jonge WJM, Dickson DPE, Johnson CE, Tinus AMC. Variation of the Néel temperature of the one-dimensional antiferromagnet  $K_2FeF_5$  with applied field. *Journal of Physics C: Solid State Physics.* 1982;15(19):4141.
23. Christian AB, Hunt CD, Neumeier JJ. Local and long-range order and the influence of applied magnetic field on single-crystalline  $NiSb_2O_6$ . *Physical Review B.* 2017;96(2):024433.

24. Melcher RL, Wallace WD. Attempt to find a magnetic field dependence of the Néel temperature of chromium. *Solid State Communications*. 1970;8(19):1535–1538.
25. Barak Zvi, Fawcett E, Feder D, Lorincz G, Walker MB. Experimental and theoretical investigation of the magnetic phase diagram of chromium. *Journal of Physics F: Metal Physics*. 1981;11.4:915.
26. Inden G. The role of magnetism in the calculation of phase diagrams. *Physica B+C*. 1981;103(1):82–100.
27. Hillert M, Jarl M. A model for alloying in ferromagnetic metals. *Calphad*. 1978;2(3):227–238.
28. Xiong W, Hedström P, Selleby M, Odqvist J, Thuvander M, Chen Q. An improved thermodynamic modeling of the Fe-Cr system down to zero kelvin coupled with key experiments. *Calphad*. 2011;35(3):355–366
29. Aristeidakis JS, Haidemenopoulos GN. Composition and processing design of medium-Mn steels based on CALPHAD, SFE modeling, and genetic optimization. *Acta Materialia*. 2020;193:291–310.
30. Arajs S, Colvin RV. Ferromagnetic-paramagnetic transition in iron. *Journal of Applied Physics*. 1964;35(8):2424–2426.
31. Stormvinter A, Borgenstam A, Ågren J. Thermodynamically based prediction of the martensite start temperature for commercial steels. *Metallurgical and Materials Transactions A*. 2012;43(10):3870–3879.
32. Lloyd JT, Field DM, Limmer KR. A four parameter hardening model for TWIP and TRIP steels. *Materials & Design*. 2020;194:108878.
33. Pisarik ST, Van Aken DC. Thermodynamic driving force of the  $\gamma \rightarrow \epsilon$  transformation and resulting Ms temperature in high-Mn steels. *Metall Mater Trans A*. 2016;47:1009–1018. doi.org/10.1007/s11661-015-3265-x.
34. Arajs S, Colvin RV, Chessin H, Peck JM. Paramagnetic behavior of iron-rich iron-vanadium alloys. *Journal of Applied Physics*. 1962;33(3):1353–1354.
35. TC-Python [accessed 2022 July 29]. <https://thermocalc.com/products/software-development-kits/tc-python/>.
36. TCFE10: TCS steel and Fe-alloys database version 10 [accessed 2021 July 1]. <https://thermocalc.com/content/uploads/Documentation/Databases/Thermodynamic/tcfe10-technical-info.pdf>.

## **Appendix A. MAGNETS.py\***

---

---

This appendix appears as a pdf attached to the report.

## **Appendix B. MAGNETS\_examples.ipynb\***

---

---

This appendix appears as a pdf attached to the report.

## List of Symbols, Abbreviations, and Acronyms

---

$\alpha$	iron-based ferrite/BCC phase
at	atomic fraction
at%	atomic percent
AFM	antiferromagnetic, antiferromagnetism
API	Application Programming Interface
BCC	body-centered cubic
$\beta$	magnetic moment
$C$	Curie constant
CALPHAD	CALculation of PHAsE Diagrams
Ch	chromium
Co	cobalt
Cr	chromium
CSV	comma-separated value
$dG$	free energy of phases
$\epsilon$	iron-based HCP phase
FCC	face-centered cubic
Fe	iron
Gd	gadolinium
H	applied field
HCP	hexagonal close-packed
$\gamma$	iron-based austenite/FCC phase
IHJ	Inden–Hillert–Jarl
j	Weiss molecular field theory parameter
k	Boltzmann's constant
M	magnetization

$M_0$	saturation magnetization
$M_{fi}$	field-induced magnetism
Mn	manganese
Mo	molybdenum
$M_s$	martensite start temperature
$M_{zf}$	zero-field magnetism
$N_A$	Avogadro's number
Ni	
$\theta$	paramagnetic Curie temperature
RGB	red–green–blue
SFE	stacking fault energy
T	Tesla
$T$	temperature
$T_C$	Curie temperature
$T_N$	Néel temperature
WMFT	Weiss Molecular Field Theory
wt	weight fraction
wt%	weight percent
$x$	composition
V	vanadium

1 DEFENSE TECHNICAL  
(PDF) INFORMATION CTR  
DTIC OCA

1 DEVCOM ARL  
(PDF) FCDD RLD DCI  
TECH LIB

10 DEVCOM ARL  
(PDF) FCDD RLR E  
C VARANASI  
FCDD RLW MB  
E HERNANDEZ  
D MAGAGNOSC  
FCDD RLW MF  
H MURDOCH  
D FIELD  
A GIRI  
M WALOCK  
FCDD RLW TE  
J LLOYD  
FCDD RLW TB  
J CLAYTON  
FCDD RLW TA  
M COPPINGER